Loss of the voltage-gated proton channel Hv1 decreases insulin secretion and leads to hyperglycemia and glucose intolerance in mice

Received for publication, August 5, 2019, and in revised form, January 16, 2020 Published, Papers in Press, January 16, 2020, DOI 10.1074/jbc.RA119.010489

Huimin Pang[‡], Xudong Wang[‡], Shiqun Zhao[§], Wang Xi[‡], Jili Lv[‡], Jiwei Qin[‡], Qing Zhao[‡], Yongzhe Che[¶], Liangyi Chen[§1], and Shu Jie Li[‡2]

From the [‡]Department of Biophysics, School of Physics Science, Key Laboratory of Bioactive Materials, Ministry of Education, Nankai University, Tianjin 300071, China, the [§]Institute of Molecular Medicine, Peking University, Beijing 100871, China, and the [¶]School of Medicine, Nankai University, Tianjin 300071, China

Edited by Jeffrey E. Pessin

Insulin secretion by pancreatic islet β-cells is regulated by glucose levels and is accompanied by proton generation. The voltage-gated proton channel Hv1 is present in pancreatic β-cells and extremely selective for protons. However, whether Hv1 is involved in insulin secretion is unclear. Here we demonstrate that Hv1 promotes insulin secretion of pancreatic β-cells and glucose homeostasis. Hv1-deficient mice displayed hyperglycemia and glucose intolerance because of reduced insulin secretion but retained normal peripheral insulin sensitivity. Moreover, Hv1 loss contributed much more to severe glucose intolerance as the mice got older. Islets of Hv1-deficient and heterozygous mice were markedly deficient in glucose- and K^+-induced insulin secretion. In perifusion assays, Hv1 deletion dramatically reduced the first and second phase of glucose-stimulated insulin secretion. Islet insulin and proinsulin content was reduced, and histological analysis of pancreas slices revealed an accompanying modest reduction of β-cell mass in Hv1 knockout mice. EM observations also indicated a reduction in insulin granule size, but not granule number or granule docking, in Hv1-deficient mice. Mechanistically, Hv1 loss limited the capacity for glucose-induced membrane depolarization, accompanied by a reduced ability of glucose to raise Ca^{2+} levels in islets, as evidenced by decreased durations of individual calcium oscillations. Moreover, Hv1 expression was significantly reduced in pancreatic β-cells from streptozotocin-induced diabetic mice, indicating that Hv1 deficiency is associated with β-cell dysfunction and diabetes. We conclude that Hv1 regulates insulin secretion and glucose homeostasis through a mechanism that depends on intracellular Ca^{2+} levels and membrane depolarization.

Insulin secretion by pancreatic β-cells is precisely regulated by glucose homeostasis. Defective insulin secretion because of β-cell loss or dysfunction causes type 1 and type 2 diabetes (T2D),[3] respectively (1). In the presence of high concentrations of glucose, β-cells metabolize glucose and generate ATP, which closes ATP-dependent K^+ channels and results in membrane depolarization and the subsequently increased intracellular Ca^{2+} that triggers insulin granule release (1).

There are two different time stages in insulin secretion in humans (2) and rodents (3, 4), including a fast transient first phase and a slow sustained second phase. In patients with T2D, the first phase has almost disappeared, and the second phase is markedly decreased (5). Multiple factors influence the biphasic nature of GSIS, including intracellular Ca^{2+} levels, distinct pools of insulin granules, and metabolic signaling (6–8). A decrease in insulin secretion may be caused by a single- or multiple-step defect in the trafficking cycle of insulin granules, including granule biogenesis from the trans-Golgi network, subsequent maturation, recruitment to the plasma membrane, exocytosis, and endocytosis.

Glucose metabolism by pancreatic β-cells accompanies proton generation, which implies a mechanism of intracellular pH-regulation behind insulin release stimulated by the sugar (9). Manipulating intracellular as well as extracellular pH could affect the insulin secretion process, which is associated with changes in membrane potential, ionic flux, and insulin release (9–11). Barg *et al.* (12) showed that the acidic pH in insulin granules might regulate priming of the granules for secretion, a process involving pairing of SNAREs on vesicles and target membranes to establish fusion competence.

The voltage-gated proton channel Hv1 is extremely selective for protons and has no detectable permeability to other cations (13, 14). Hv1 is activated at depolarizing voltages and sensitive to the membrane pH gradient (13, 14). Hv1 sustains calcium entry in neutrophils and maintains intracellular alkalization to support the activity of human spermatozoa (15, 16). In our previous study, we identified that Hv1 is present in human and rodent pancreatic islet β-cells as well as β-cell lines (17). How-

This work was partly supported by National Natural Science Foundation of China Grant 31271464. The authors declare that they have no conflicts of interest with the contents of this article.

[1] To whom correspondence may be addressed. E-mail: lychen@pku.edu.cn.
[2] To whom correspondence may be addressed: Dept. of Biophysics, Key Laboratory of Bioactive Materials, Ministry of Education, Nankai University, 94 Weijin Rd., Nankai District, Tianjin 300071, China. Tel./Fax: 86-22-2350-6973; E-mail: shujieli@nankai.edu.cn.

[3] The abbreviations used are: T2D, type 2 diabetes; GSIS, glucose-stimulated insulin secretion; IPGTT, i.p. glucose tolerance test; IPITT, i.p. insulin tolerance test; AUC, area under the curve; TEM, transmission EM; GSCa, glucose-stimulated calcium; PMA, phorbol 12-myristate 13-acetate; KRBH, Krebs–Ringer bicarbonate HEPES; pHc, cytosolic pH; STZ, streptozotocin; HOMA-IR, homeostasis model assessment insulin resistance; VSOP, voltage sensor domain-only protein; Hv1, hydrogen voltage-gated channel 1.

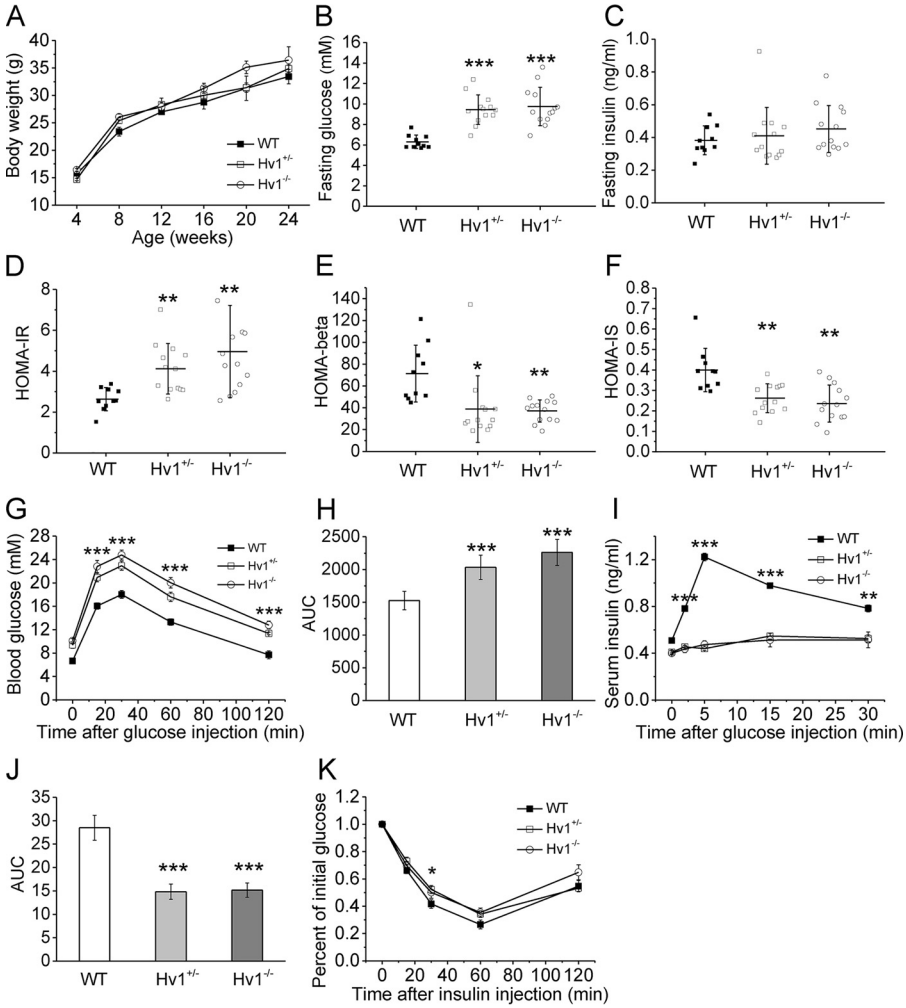

Figure 1. Mice deleted for Hv1 display hyperglycemia and impaired glucose tolerance because of reduced insulin secretion. *A*, body weight change of $Hv1^{-/-}$, $Hv1^{+/-}$, and WT mice ($n = 24$/genotype). Data are means ± S.D. *B* and *C*, basal blood glucose (*B*) and corresponding serum insulin (*C*) concentrations after fasting for 6 h in 4-month-old $Hv1^{-/-}$, $Hv1^{+/-}$, and WT mice ($n = 13$ for $Hv1^{-/-}$ and $Hv1^{+/-}$ and $n = 10$ for WT). Data are means ± S.D. ***, $p < 0.001$; $Hv1^{-/-}$ or $Hv1^{+/-}$ *versus* WT. *D–F*, HOMA parameters calculated from basal blood glucose (*B*) and corresponding serum insulin (*C*) concentrations. Data are means ± S.D. *, $p < 0.05$; **, $p < 0.001$; $Hv1^{-/-}$ or $Hv1^{+/-}$ *versus* WT. HOMA-IR was calculated as follows: fasting glucose (millimoles per liter) × fasting insulin (milliunits per liter) / 22.5. Homeostasis model assessment insulin sensitivity is the reciprocal of HOMA-IR. Homeostasis model assessmen islet β cell insulin secretory function was calculated as follows: 20 × fasting insulin (milliunits per liter) / (fasting glucose (millimoles per liter) − 3.6). *G* and *H*, Blood glucose levels measured in whole blood following i.p. injection of glucose (2 g/kg of body weight) in $Hv1^{-/-}$, $Hv1^{+/-}$, and WT mice (*G*) and AUC (*H*) ($n = 12$/genotype). Data are means ± S.E. ***, $p < 0.001$; $Hv1^{-/-}$ *versus* WT. *I* and *J*, insulin concentrations measured in sera of $Hv1^{-/-}$, $Hv1^{+/-}$, and WT mice following i.p. glucose challenge (2 g/kg of body weight) (*I*) and AUC (*J*) ($n = 8$/genotype). Data are means ± S.E. **, $p < 0.01$; ***, $p < 0.001$; $Hv1^{-/-}$ or $Hv1^{+/-}$ *versus* WT. *K*, blood glucose levels measured in whole blood following i.p. insulin injection (1 unit/kg of body weight) in $Hv1^{-/-}$, $Hv1^{+/-}$, and WT mice ($n = 12$/genotype). Data are means ± S.E. *, $p < 0.05$; $Hv1^{-/-}$ *versus* WT.

ever, the regulatory mechanism of Hv1 for insulin secretion of pancreatic islet β-cells is not known.

In this study, we discovered a regulatory mechanism for Hv1 in the modulation of β-cell insulin secretory function. Our *in vivo* and *in vitro* studies demonstrated that Hv1-deficient mice exhibit hyperglycemia and glucose intolerance because of abnormally decreased insulin secretion. These data provide direct genetic evidence that Hv1 regulates biphasic insulin secretion and glucose homeostasis in mice, implying a potential link between Hv1 and the pathogenesis of diabetes mellitus.

Results

Hv1-deficient mice exhibit hyperglycemia and impaired glucose tolerance because of reduced insulin secretion

To assess the effect of Hv1 knockout on glucose homeostasis, glucose and insulin levels were measured in 4-month-old mice in a fasted state. The body weight curves of control (WT, $Hv1^{+/+}$), heterozygous ($Hv1^{+/-}$), and homozygous (KO, $Hv1^{-/-}$) littermates were almost similar (Fig. 1*A*), but the blood glucose levels in the fasted state were markedly higher in heterozygous (9.45 ± 0.39 mmol/liter, $n = 13$, $p < 0.001$) and KO (9.75 ± 0.52 mmol/liter, $n = 13$, $p < 0.001$) mice compared with WT mice (6.3 ± 0.2 mmol/liter, $n = 10$) (Fig. 1*B*), whereas the fasting insulin levels in these three genotypes were not significantly different (Fig. 1*C*). To qualitatively estimate the effect of Hv1 on insulin resistance, insulin sensitivity, and β-cell function, we calculated Homeostasis model assessment insulin resistance (an index of insulin resistance), HOMA-β (an index of insulin secretory function), and HOMA-IS (an index of insulin sensitivity) from the corresponding glucose and insulin levels (18). The results showed that loss of Hv1 had a tendency for insulin resistance (Fig. 1*D*) because of decreased insulin sensitivity (Fig.

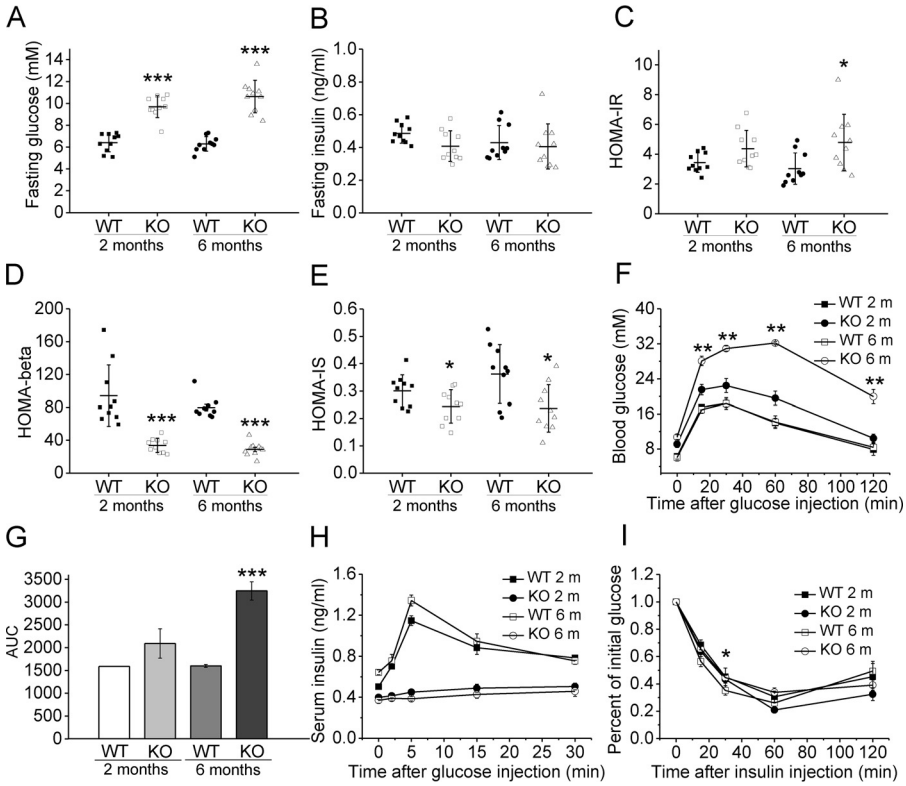

Figure 2. Age-dependent glucose intolerance in Hv1-deficient mice. *A* and *B*, basal blood glucose (*A*) and corresponding serum insulin (*B*) concentrations after fasting for 6 h in 2- and 6-month-old KO and WT mice ($n = 10$/genotype). Data are means ± S.D. ***, $p < 0.001$; KO *versus* corresponding WT. *C–E*, HOMA-IR (*C*), HOMA-β (*D*) and HOMA-IS (*E*) parameters calculated from basal blood glucose (*A*) and corresponding serum insulin (*B*) concentrations. Data are means ± S.D. *, $p < 0.05$; ***, $p < 0.001$; KO *versus* corresponding WT. *F* and *G*, blood glucose levels measured in whole blood following i.p. injection of glucose (2 g/kg of body weight) in 2- and 6-month-old KO and WT mice (*F*) and AUC (*G*) ($n = 12$/genotype). 6-month-old KO mice show more serious glucose intolerance than 2-month-old KO mice. Data are means ± S.E. **, $p < 0.01$; ***, $p < 0.001$; KO *versus* corresponding WT. *H*, insulin concentrations measured in sera of KO and WT mice following i.p. glucose challenge (2 g/kg of body weight) in 2- and 6-month-old KO and WT mice ($n = 8$/genotype). Data are means ± S.E. *I*, blood glucose levels measured in whole blood following i.p. insulin injection (1 unit/kg of body weight) in 2- and 6-month-old KO and WT mice ($n = 12$/genotype). Data are means ± S.E. *, $p < 0.05$ *versus* corresponding WT.

1*F*). The calculated results also showed that Hv1 deficiency significantly affected β-cell secretory function (Fig. 1*E*), which is involved in hyperglycemia.

To evaluate the impact of Hv1 on disposal of a glucose load, i.p. glucose tolerance tests (IPGTTs) were performed. Compared with WT mice, KO and heterozygous mice 4 months of age showed significantly higher glucose levels following an i.p. glucose load (2 g/kg of body weight) (Fig. 1, *G* and *H*). The corresponding serum insulin levels were significantly lower in Hv1-deficient mice throughout the IPGTT after glucose challenge compared with WT mice, providing evidence for an insulin secretion defect in response to glucose (Fig. 1, *I* and *J*). Thus, Hv1-deficient mice exhibit impairment in their ability to dispose of a glucose load because of an insulin secretion defect.

To explore the possibility that the observed glucose intolerance was a result of peripheral insulin resistance, we performed i.p. insulin tolerance tests (IPITTs) in KO mice 4 months of age. We found that insulin administration lowered blood glucose levels in WT and Hv1-deficient mice to a similar extent, indicating that Hv1 deficiency does not impair peripheral insulin sensitivity (Fig. 1*K*). Taken together, these data are compatible with the notion that loss of Hv1 results in impaired glucose tolerance because of an insulin secretion defect *in vivo*.

Hv1 deletion mice display an age-dependent development in glucose intolerance

To examine the age-dependent effect of Hv1 on glucose tolerance and insulin resistance, we performed IPGTTs and IPITTs in 2- and 6 month-old WT and KO mice as described above. The fasting blood glucose levels in KO mice (9.7 ± 0.31 mmol/liter, $n = 10$, $p < 0.001$ for 2 month-old mice; 10.63 ± 0.47 mmol/liter, $n = 10$, $p < 0.001$ for 4-month-old mice) were also significantly higher than in WT mice (6.42 ± 0.27 mmol/liter, $n = 10$ for 2 month-old mice; 6.3 ± 0.2 mmol/liter, $n = 10$ for 4 month-old mice) (Fig. 2*A*). There was almost no difference in the blood insulin levels in the fasted state between 2- and 6-month-old KO mice (Fig. 2*B*). The HOMA parameters calculated from the corresponding blood glucose and insulin levels showed a potential tendency for insulin resistance in 2- and 6-month-old KO mice (Fig. 2, *C* and *E*) and significant dysfunction of β-cells (Fig. 2*D*). The IPGTT showed more serious glucose intolerance in 6-month-old KO mice than in 2-month-old KO mice (Fig. 2, *F* and *G*), whereas WT mice showed no glucose intolerance at different ages. Although serum insulin levels in response to glucose in both 2- and 6-month-old KO mice were markedly lower than in WT mice (Fig. 2*H*), the IPITT showed no obvious insulin resistance in 2- and 6-month-old

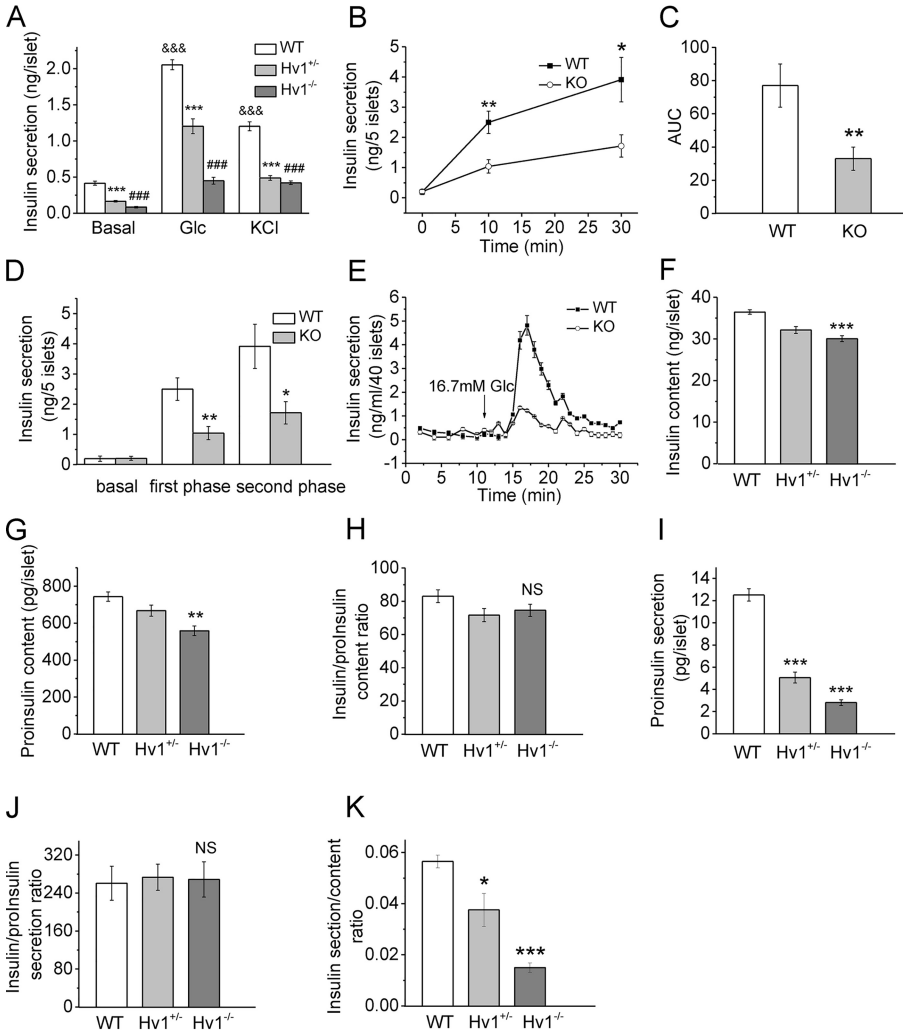

Figure 3. Knockout of Hv1 inhibits insulin secretion in isolated islets. *A*, glucose- and KCl-induced insulin secretion from isolated islets of Hv1$^{-/-}$, Hv1$^{+/-}$, and WT mice ($n = 8$/genotype). Data are means ± S.E. ***, $p < 0.001$, Hv1$^{+/-}$ *versus* corresponding WT; ###, $p < 0.001$, Hv1$^{-/-}$ *versus* corresponding WT; &&&, $p < 0.001$, glucose (*Glc*) or KCl *versus* basal for WT. Basal, 2.8 mM glucose; glucose, 16.7 mM glucose; KCl, 60 mM KCl. *B–D*, time-dependent GSIS stimulated by 16.7 mM glucose (*B*), AUC (*C*), and amounts of first- and second-phase insulin secretion (*D*) from isolated islets of WT and KO mice ($n = 6$/genotype). Data are means ± S.E. *, $p < 0.05$; **, $p < 0.01$; *versus* corresponding WT. *E*, perifusion assays for the kinetics of insulin secretion in isolated islets of KO and WT mice ($n = 8$/genotype). The *arrow* indicates the time of 16.7 mM glucose addition. *F* and *G*, insulin (*F*) and proinsulin (*G*) content under basal conditions in isolated islets from Hv1$^{-/-}$, Hv1$^{+/-}$, and WT mice ($n = 8$/genotype). Data are means ± S.E. **, $p < 0.01$; ***, $p < 0.001$; Hv1$^{-/-}$ *versus* WT. *H*, ratio of insulin to proinsulin content of isolated islets of Hv1$^{-/-}$, Hv1$^{+/-}$, and WT mice under basal conditions ($n = 8$/genotype). Data are means ± S.E. *NS*, no significance, *versus* WT. *I*, proinsulin secretion at 16.7 mM glucose from isolated islets of Hv1$^{-/-}$, Hv1$^{+/-}$, and WT mice ($n = 8$/genotype). Data are means ± S.E. ***, $p < 0.001$; Hv1$^{-/-}$ or Hv1$^{+/-}$ *versus* WT. *J* and *K*, ratio of insulin to proinsulin secretion (*J*) and of insulin secretion to insulin content (*K*) of isolated islets of Hv1$^{-/-}$, Hv1$^{+/-}$, and WT mice at 16.7 mM glucose ($n = 8$/genotype). Data are means ± S.E. *, $p < 0.05$; ***, $p < 0.001$; Hv1$^{-/-}$ or Hv1$^{+/-}$ *versus* WT.

KO mice (Fig. 2*I*), indicating that hyperglycemia in Hv1-deficient mice is not caused by abnormal insulin sensitivity or T2D.

Reduced insulin secretion of islets from Hv1-deficient mice

To delineate the role of Hv1 in insulin secretion, we performed insulin secretion assays using isolated islets from WT, Hv1$^{+/-}$, and KO mice. As shown in Fig. 3*A*, 16.7 mM glucose–induced insulin secretion was significantly reduced by 51% ($n = 8$, $p < 0.001$) and 78% ($n = 8$, $p < 0.001$) in Hv1$^{+/-}$ and KO islets compared with WT islets ($n = 8$). Basal insulin secretion (at 2.8 mM glucose) in Hv1$^{+/-}$ and KO islets was also significantly reduced by 60% ($n = 8$, $p < 0.001$) and 80% ($n = 8$, $p < 0.001$) compared with WT islets ($n = 8$). Direct depolarization elicited by an increase in extracellular K^+ (60 mM KCl) also reduced insulin secretion by 59% ($n = 8$, $p < 0.001$) and 65% ($n = 8$, $p < 0.001$) in Hv1$^{+/-}$ and KO islets compared with WT islets ($n = 8$) (Fig. 3*A*), indicating that knockout of Hv1 prevents K^+-induced insulin secretion in pancreatic β-cells. Together, these data indicate that loss of Hv1 in islets inhibits insulin secretion.

Next we examined Hv1 function in biphasic GSIS by static incubation and perifusion assays from pancreatic islets. In static incubation assays, we measured the amounts of first-phase (within the first 10 min) and second-phase (within the following 20 min) insulin secretion stimulated by 16.7 mM glucose in isolated islets in WT and KO mice. As shown in Fig. 3*B*, Hv1 deficiency strikingly impaired both first- and second-phase in GSIS. In an area under the curve (AUC) analysis (Fig. 7*B*), the AUC in KO islets was significantly decreased by 60% ($p < 0.05$) compared with that in the WT, which was consistent

with Fig. 3*A*. Insulin secretion in the time windows of 0–10 min and 10–20 min in Fig. 3*B* was calculated as the first phase and second phase (Fig. 3*D*). The same results also occurred in perifusion assays. GSIS in KO mice was markedly decreased in the first and second phase (Fig. 3*E*). Our results clearly demonstrate that loss of Hv1 inhibits insulin secretion in the first and second phase.

We also investigated the effect of Hv1 on insulin granule biogenesis. Insulin and proinsulin content in KO islets was reduced by 17% ($n = 8$, $p < 0.001$) and 25% ($n = 8$, $p < 0.01$), respectively, compared with WT islets ($n = 8$) under basal conditions (2.8 mM glucose) (Fig. 3, *F* and *G*). The ratio of insulin to proinsulin content, however, was indistinguishable between KO and WT islets (Fig. 3*H*), suggesting that insulin synthesis, but not insulin maturation, is abnormal in KO islets. Proinsulin secretion was barely detectable under basal conditions (2.8 mM glucose) in WT, $Hv1^{+/-}$, and KO islets (data not shown). In the presence of 16.7 mM glucose, proinsulin secretion was reduced by 59% ($n = 8$, $p < 0.001$) and 78% ($n = 8$, $p < 0.001$) in heterozygous and KO islets compared with WT islets ($n = 8$) (Fig. 3*I*). However, the ratio of insulin to proinsulin secretion in $Hv1^{+/-}$ and KO islets in the presence of 16.7 mM glucose was not different from WT islets (Fig. 3*J*). The ratio of insulin secretion to insulin content was remarkably reduced in islets of $Hv1^{+/-}$ and KO mice compared with WT mice (Fig. 3*K*). These results suggest that no significant accumulation of proinsulin occurred in KO islets and that the significant reduction in insulin secretion is not completely caused by insulin granule biogenesis.

Hv1 deficiency reduces β-cell mass and pancreatic insulin content

To determine whether Hv1 deletion affects islet development, we conducted immunohistological studies. Morphometric analysis of pancreatic sections from WT, $Hv1^{+/-}$, and KO mice at 4 months of age showed relatively normal islet architecture in each case, with β-cells concentrated in the core and α-cells located mainly in the periphery (Fig. 4*A*), whereas the morphology of isolated islets cultured overnight from KO mice was not overtly different from WT islets (data not shown). On the other hand, the number of the isolated islets per pancreas was not significantly different between WT and KO mice (data not shown), which is consistent with the result from the immunohistochemical analysis (Fig. 4*B*). However, the average islet size, calculated from isolated islets (Fig. 4*C*), and islet area to total pancreas area (Fig. 4*D*), analyzed by immunohistochemistry of pancreatic sections, were decreased in KO mice compared with WT and $Hv1^{+/-}$ mice.

Quantification of total β-cell mass displayed a genotype-dependent difference. β-Cell mass was decreased by 13% ($n = 6$, $p < 0.05$) in KO mice compared with WT mice ($n = 6$), as measured by morphometric analysis of insulin-positive islet cells (Fig. 4*E*). Total pancreatic insulin content in KO mice was also decreased by 11% ($n = 6$, $p < 0.05$) (Fig. 4*F*), the same as the result obtained from isolated islets (Fig. 3*F*). These results show that KO mice have sufficient β-cells and insulin, indicating that the *in vivo* phenotype is not due to gross developmental defects.

Hv1 deficiency affects the size of insulin granules but not the number and docking of vesicles

Insulin is stored in large dense-core secretory granules in β-cells and released via granule exocytosis upon stimulation. The correct size, number, and docking to the cell membrane of insulin granules are necessary for insulin secretion in β-cells (19, 20). We used TEM to investigate whether loss of Hv1 disturbed vesicle distribution in β-cells. The ratios of small vesicles (<300 nm) and large vesicles (>400 nm) were increased by 4-fold and decreased by 47% in KO mice compared with WT mice, respectively, but the ratio of the medium vesicles (300–400 nm) showed no significant difference (Fig. 4, *G* and *H*). However, the total number of vesicles in β-cells in KO mice was the same as that in WT mice (Fig. 4*I*). This result might explain why there is a difference in insulin content between KO and WT mice (Fig. 3*F*). Docking of insulin granules plays an important role in regulating insulin secretion (20). A detailed quantitative electron microscopy analysis of β-cells was performed to study docked granules. The number of secretory granules close to (<100 nm) the cell membrane in β-cells in KO mice was similar to that in WT mice (Fig. 4*J*), indicating that loss of Hv1 does not affect granule docking in β-cells.

We further investigated the expression of syntaxin1A (Stx1a), vesicle-associated membrane protein 2 (VAMP2), and synaptotagmin-7 (Syt7), proteins related to insulin secretion, in isolated islets from WT and KO mice (21, 22). Their expression levels were slightly down-regulated, as determined by Western blotting (Fig. 4*K*). The reduced membrane fusion protein suggests that lack of Hv1 may affect fusion of insulin granules with the plasma membrane.

Hv1 deficiency affects glucose-induced Ca^{2+} oscillation and limits membrane depolarization

Glucose stimulates insulin secretion by induction of Ca^{2+}-dependent electrical activity, which triggers exocytosis of insulin granules. Glucose-stimulated calcium (GSCa) signaling and GSIS show similar trajectories (23). Thus, GSCa can be used to assess the physiological response of islets to glucose stimulation. Ca^{2+} imaging is advantageous because it provides high temporal precision of real-time changes in response to stimuli at the level of the individual islet (24). The data presented in Fig. 5, *A* and *B*, are representative curves and average graphs of GSCa over time for islets isolated from WT and KO mice, respectively. The baseline, amplitude, timing, and duration of the biphasic response to glucose stimulation were calculated according to Fig. 5*A*. As shown in Fig. 5*C*, the mean value of cellular Ca^{2+} levels for baseline under basal conditions was increased by 12% in KO islets compared with the WT, suggesting that elevated $[Ca^{2+}]_i$ under low glucose does not lead to increased insulin release. After stimulation, both WT and KO islets displayed a large spike in calcium influx, and the mean values for peaks showed difference between KO and WT islets (Fig. 5*D*). However, the mean duration was decreased by 32% in KO islets compared with the WT (Fig. 5*E*), and the time to peak was decreased by 31% (Fig. 5*F*),

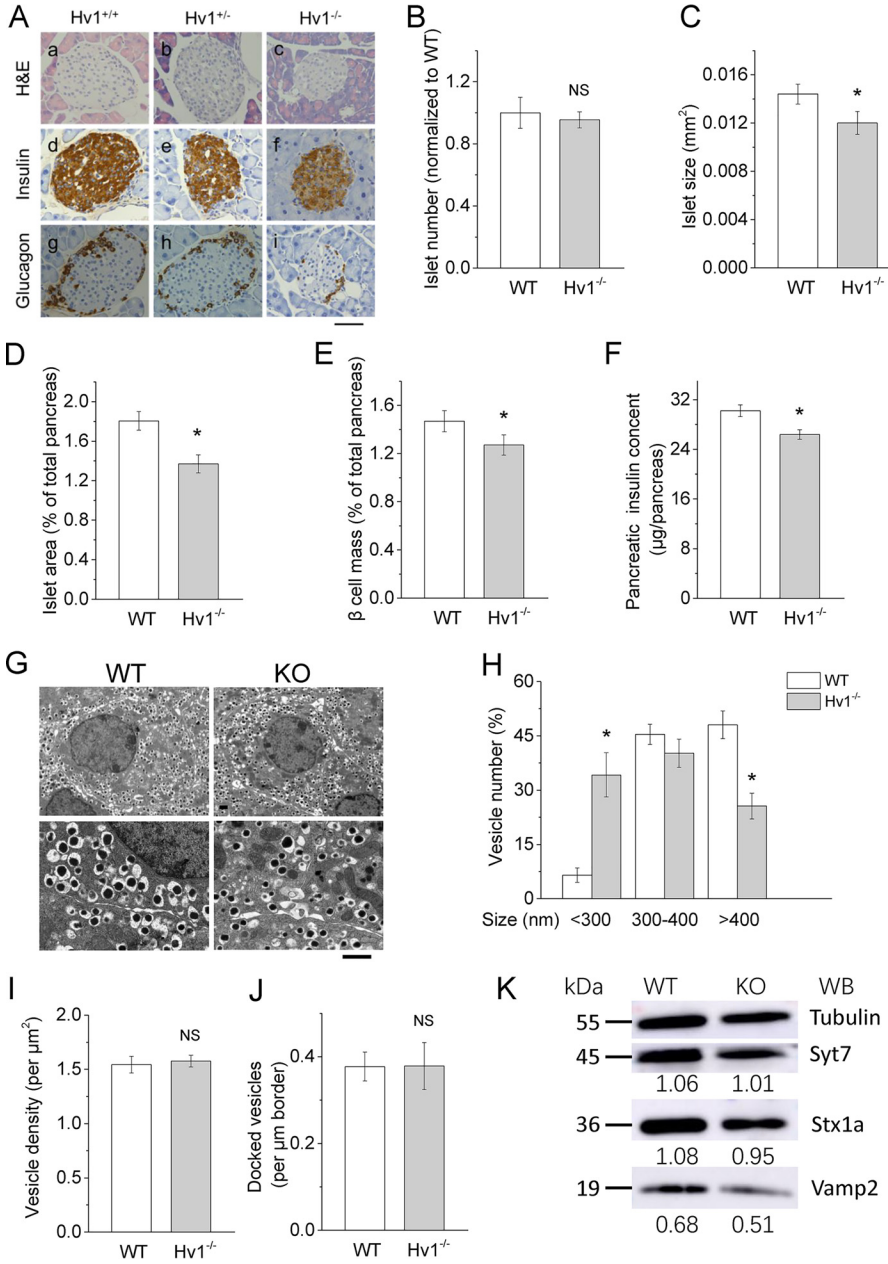

Figure 4. Effects of Hv1 on β-cell mass, size and number of insulin granules, and docking of vesicles. *A*, immunohistochemical analysis of 4-month-old WT, $Hv1^{+/-}$, and $Hv1^{-/-}$ islets using anti-insulin and anti-glucagon antibodies and representative images of H&E–, anti-insulin–, and anti-glucagon antibody–stained pancreatic sections from 4-month-old WT, $Hv1^{+/-}$, and $Hv1^{-/-}$ mice. *Scale bar* = 50 μm. *B* and *C*, relative islet number based on immunohistochemical analysis of pancreatic sections (*B*) and islet size calculated by isolated islet area (*C*) in 4-month-old WT and $Hv1^{-/-}$ mice ($n = 6$/genotype). Data are means ± S.E. *NS*, no significance; *, $p < 0.05$ *versus* WT. *D*, relative islet area of 4-month-old WT and $Hv1^{-/-}$ mice analyzed by immunohistochemistry of pancreatic sections ($n = 6$/genotype). Data are means ± S.E. *, $p < 0.05$ *versus* WT. *E*, β-cell mass of 4-month-old WT and $Hv1^{-/-}$ mice based on immunostaining of pancreatic sections ($n = 6$/genotype). Relative β-cell mass was determined as a ratio of total insulin-positive area to total pancreatic area. Twenty to thirty sections per pancreas were analyzed. Data are presented as mean ± S.E. *, $p < 0.05$ *versus* WT. *F*, pancreatic insulin content ($n = 6$/genotype). Data are mean ± S.E. *, $p < 0.05$ *versus* WT. *G*, representative TEM images of β-cells from 4-month-old WT and KO mice. *Scale bar* = 2 μm. *H*, relative size distribution of vesicles in β-cells based on TEM images. The size of vesicles in KO mice is smaller than in WT mice ($n = 50$/genotype). Data are means ± S.E. *, $p < 0.05$ *versus* WT. *I*, vesicle density in pancreatic β-cells of 4-month-old WT and KO mice analyzed by TEM images ($n = 50$/genotype). Data are means ± S.E., *versus* WT. *J*, number of vesicles docked onto the cytoplasmic membrane in β-cells of WT and KO islets from TEM-based analysis ($n = 50$/genotype). Data are means ± S.E., *versus* WT. *K*, expression of tubulin, Stx1a, Syt7, and Vamp2 in isolated islets from WT and KO mice, as determined by Western blotting.

suggesting that loss of Hv1 results in dissociation between calcium signaling and GSIS.

In pancreatic β-cells, the increase in $[Ca^{2+}]_i$ occurs with Ca^{2+} entry across voltage-sensitive Ca^{2+} channels activated by membrane depolarization (6). To confirm whether the change in calcium signaling by knockout of Hv1 is coupled to membrane polarization, the membrane potential difference was monitored with DiBAC4(3) fluorescence. As shown in Fig. 5, *G* and *H*, isolated islet β-cells from WT mice were depolarized significantly more than isolated islet β-cells from KO mice after glucose stimulation, indicating that Hv1 deficiency impairs glucose-induced membrane depolarization. Thus, the reduction in insulin secretion by Hv1 deficiency is involve in electrical activity and $[Ca^{2+}]_i$ signaling.

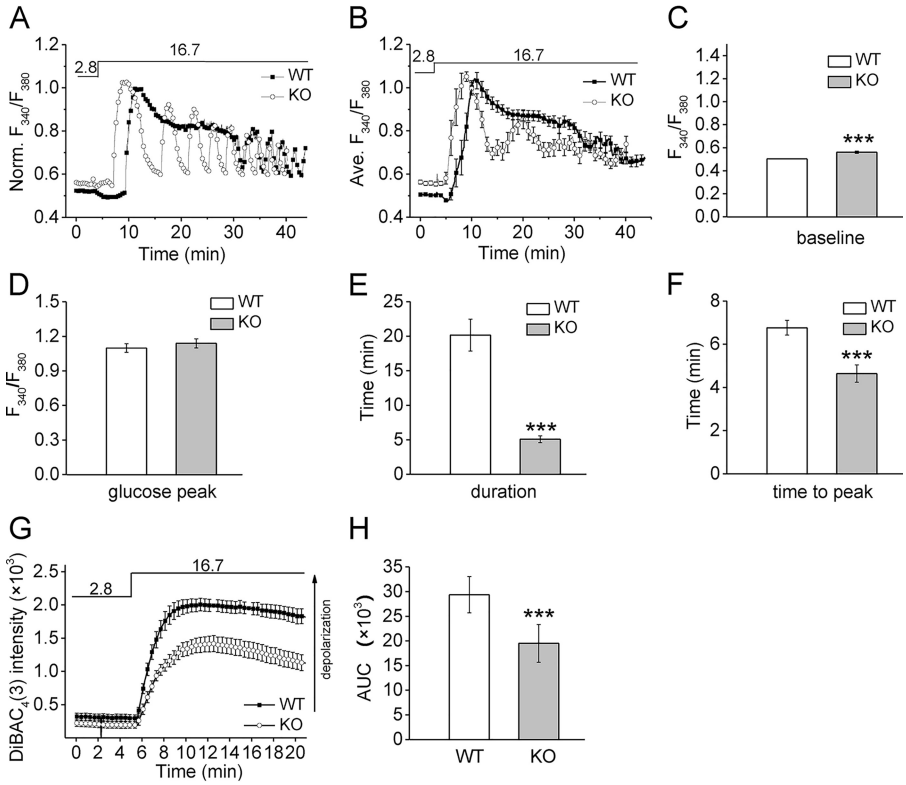

Figure 5. Deficiency of Hv1 limits membrane depolarization and results in disassociation between calcium signaling and insulin secretion. *A* and *B*, representative curves (*A*) and average traces (*B*) of GSCa from islets isolated from WT and KO mice. Cellular Ca^{2+} levels in isolated islets were measured by Fura-2 fluorescence; islets were kept at 2.8 mM glucose before switching to stimulation by 16.7 mM glucose, as indicated above the traces. *C*, mean values of cellular Ca^{2+} levels for baseline under basal conditions. Data are means ± S.E. ***, $p < 0.001$, KO *versus* WT. *D–F*, mean values of cellular Ca^{2+} levels at peaks (*D*), mean time of duration (*E*), and mean time to peak (*F*) after stimulation with glucose (final concentration, 16.7 mM). $n = 6$/genotype, 2–5 islets/experiment. Data are means ± S.E. ***, $p < 0.001$, KO *versus* WT. *G* and *H*, membrane potential changes of isolated islet β-cells during glucose stimulation were monitored by $DiBAC_4(3)$ fluorescence (*G*) and AUC (*H*). Isolated islet β-cells from WT and KO mice were kept at 2.8 mM glucose before switching to stimulation by 16.7 mM glucose, as indicated above the traces. Data are means ± S.E. ***, $p < 0.001$, KO *versus* WT.

Effect of Hv1 on cytosolic pH in pancreatic β-cells

To assess the effect of Hv1 on cytosolic pH in β-cells, cytosolic pH was evaluated by BCECF fluorescence. As shown in Fig. 6*A*, the pH in KO β-cells was lower about 0.1 than that in WT β-cells at both 2.8 and 16.7 mM glucose conditions. When we changed the glucose concentration from 2.8 to 16.7 mM, there was a slight synchronous reduction in pH in WT and KO β-cells (Fig. 6*A*). The pH under steady-state basal (2.8 mM) and high-glucose (16.7 mM) conditions in KO β-cells was also slightly lower compared with the corresponding WT β-cells, but there were no significant differences between them (Fig. 6*B*), indicating that knockout of Hv1 has no a significant effect on cytosolic pH in β-cells stimulated by glucose.

PMA is a well-known activator of Hv1 and has been used extensively for Hv1 function studies (25, 26). We measured PMA-induced insulin secretion in isolated islets from WT and KO mice. As shown in Fig. 6*E*, in the presence of 5 μM PMA, insulin secretion in isolated islets from WT mice increased 6.3-fold compared with the absence of PMA, whereas insulin secretion in KO islets was significantly decreased by 61% ($p < 0.001$) compared with WT islets.

To estimate the effect of PMA on cytosolic pH, the change in fluorescence intensity at 488 nm excitement was observed with addition of PMA solution. Interestingly, the fluorescence intensity for KO β-cells was significantly reduced compared with that of the WT (Fig. 6, *C* and *D*), indicating that PMA results in a decrease in cytosolic pH.

Hv1 is down-regulated in pancreatic β-cells in STZ-induced diabetic mice

To further determine the relationship between Hv1 and insulin secretion, WT and KO mice were treated with STZ to induce diabetes. We found that fasted blood glucose levels after STZ injection in KO mice were always higher than in WT mice (Fig. 7*A*), and the IPGTT also showed higher blood glucose levels in STZ-treated KO mice than in WT mice (Fig. 7*B*). These data show that STZ-treated KO mice seem to be more sensitive to diabetes induction.

The insulin content at 2.8 mM glucose was decreased by 91% in β-cells of STZ-treated WT mice (Fig. 7*C*), whereas insulin secretion stimulated by 16.7 mM glucose was reduced by 97% (Fig. 7*D*), which is a serious insulin deficiency. Immunohistochemical analyses of islets in control and STZ-treated WT mice using anti-insulin and anti-Hv1 antibodies also showed that the mean optical density of insulin- and Hv1-positive areas in STZ-treated WT mice were decreased by 53% and 60%, respectively, compared with control mice (Fig. 7*E*), demonstrating that the expression levels of insulin and Hv1 are significantly decreased in β-cells of STZ-treated diabetes mice, as shown in Fig. 7*E*, *b* and *d*. The lower expression of Hv1 in β-cells of diabetic mice

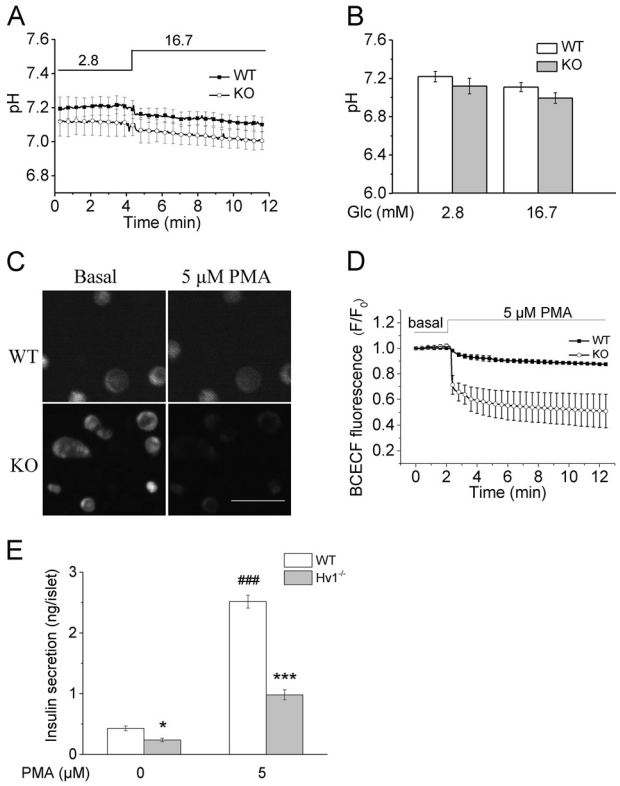

Figure 6. Effects of glucose and PMA treatment on cytosolic pH and of Hv1 on PMA-stimulated insulin secretion. *A*, effect of Hv1 on glucose-induced changes in cytosolic pH in isolated islet β-cells, determined by BCECF fluorescence. Glucose (final concentration, 16.7 mM) solution was added to the culture dishes without interruption of the recordings. *B*, cytosolic pH in β-cells isolated from WT and KO mice in the presence of 2.8 or 16.7 mM glucose (*Glc*). Data are means ± S.E. ($n = 3$/genotype). *C*, representative images of WT and KO islet β-cells loaded with BCECF dye in sodium-free solution to minimize the contribution of Na^+/H^+ exchange under basal conditions and in the presence of 5 μM PMA. *Scale bar* = 100 μm. *D*, change in fluorescence ($F488/F_0$) with time, stimulated by PMA (final concentration, 5 μM). The PMA solution was added to the culture dishes without interruption of the recordings. *E*, PMA-induced insulin secretion from isolated islets from WT and KO mice ($n = 8$/genotype). Data are means ± S.E. *, $p < 0.05$; ***, $p < 0.001$, *versus* corresponding WT; ###, $p < 0.001$ *versus* corresponding WT at 0 μM PMA.

might be due to the decrease in insulin secretion, which is consistent with the result that insulin secretion is significantly reduced in islets of $Hv1^{+/-}$ mice (Fig. 3*A*). These data suggest that Hv1 is closely related to insulin secretion.

Hv1 is down-regulated in high-glucose-induced dysfunctional β-cells

Chronic hyperglycemia can cause loss of GSIS (27). To confirm whether Hv1 is also down-regulated in dysfunctional β-cells, INS-1 (832/13) cells were incubated in 11 or 25 mM glucose, respectively, for 48 h. Following chronic incubation, insulin secretion was measured at two different concentrations of glucose (2.8 and 16.7 mM), and Hv1 expression levels were detected by immunofluorescence.

Insulin secretion in INS-1 (832/13) cells incubated chronically at 11 mM glucose was increased in response to glucose stimulation but completely unchanged with 25 mM glucose chronic incubation (Fig. 7*F*). These data are consistent with another report (27) showing that chronic high glucose causes complete loss of glucose responsiveness in INS-1 (832/13) cells. Immunofluorescence analyses of cells under 11 or 25 mM glucose chronic incubation using anti-Hv1 antibody showed that the mean fluorescence intensity in 25 mM glucose chronic incubation cells was decreased by 33.5% compared with 11 mM (Fig. 7*G*). These data demonstrate that the Hv1 expression level is also significantly decreased in the dysfunctional β-cells, which is in accordance with the STZ-induced diabetes model.

Discussion

Here we show *in vivo* that Hv1 KO and heterozygous mice display hyperglycemia and glucose intolerance because of markedly decreased insulin secretion. *In vitro*, Hv1 deficiency causes a remarkable defect in glucose- and K^+-induced insulin secretion, limiting the capacity for glucose-induced membrane depolarization that accompanies the reduced ability of glucose to raise the level of Ca^{2+} in islets, as evidenced by the decreased duration of individual calcium oscillations. These data indicate that Hv1 is required for insulin secretion and maintenance of glucose homeostasis and reveal a significant role of the proton channel in modulation of pancreatic β-cell function.

Hv1 is extremely selective for protons and has no detectable permeability to other cations (13, 14). Gating of Hv1 strongly depends on membrane depolarization and intracellular and extracellular pH (13–15, 26). The proton channel also sustains Ca^{2+} influx and enables neutrophils to generate calcium signals in response to chemoattractants, in addition to maintenance of normal cytosolic pH and membrane potential during the respiratory burst (15). Our previous work demonstrated that Hv1 mainly localizes to the insulin-containing granule membrane (17). Considering fusion of insulin-containing granules with the plasma membrane during exocytosis, Hv1 should also be in the plasma membrane in pancreatic islet β-cells. Therefore, Hv1 might be involved in regulating insulin-containing granules, cytosolic pH, membrane potential, and Ca^{2+} influx in pancreatic β-cells.

Manipulation of extracellular and intracellular pH in pancreatic islets or β-cells is associated with changes in membrane potential, ionic flux, and insulin release (9–11). Glucose-induced changes in cytosolic pH in islet β-cells are coupled to glucose metabolism and associated with triggering insulin release (10, 11). Glucose-induced priming of insulin secretion, which is thought to be mediated by the amplifying pathway (28), has been proposed to be linked to pH changes in β-cells (29). It has been suggested for decades that the proton gradients in insulin-containing granules might be involved in fusion of secretory vesicles to the target membrane (30, 31), which might affect triggering of vesicles for secretion, a process involving pairing of SNARE proteins on vesicles and target membranes to establish fusion competence (12). Dependence of insulin secretion on Hv1 activity reflects that insulin-containing granules and cytosolic pH are directly involved in secretion of secretory granules. A change in membrane potential in Hv1-deficient pancreatic β-cells under glucose stimulation condition also reflects the pH dependence of the secretory machinery as well as altered sensitivity of the secretory machinery to $[Ca^{2+}]_i$.

The fact that heterozygous mice also have hyperglycemia with a low insulin level illustrates that Hv1 is at an important control point in the metabolic pathway regulating insulin secretion and that relatively small changes in Hv1 activity are likely to have important effects on insulin secretion. Similar effects

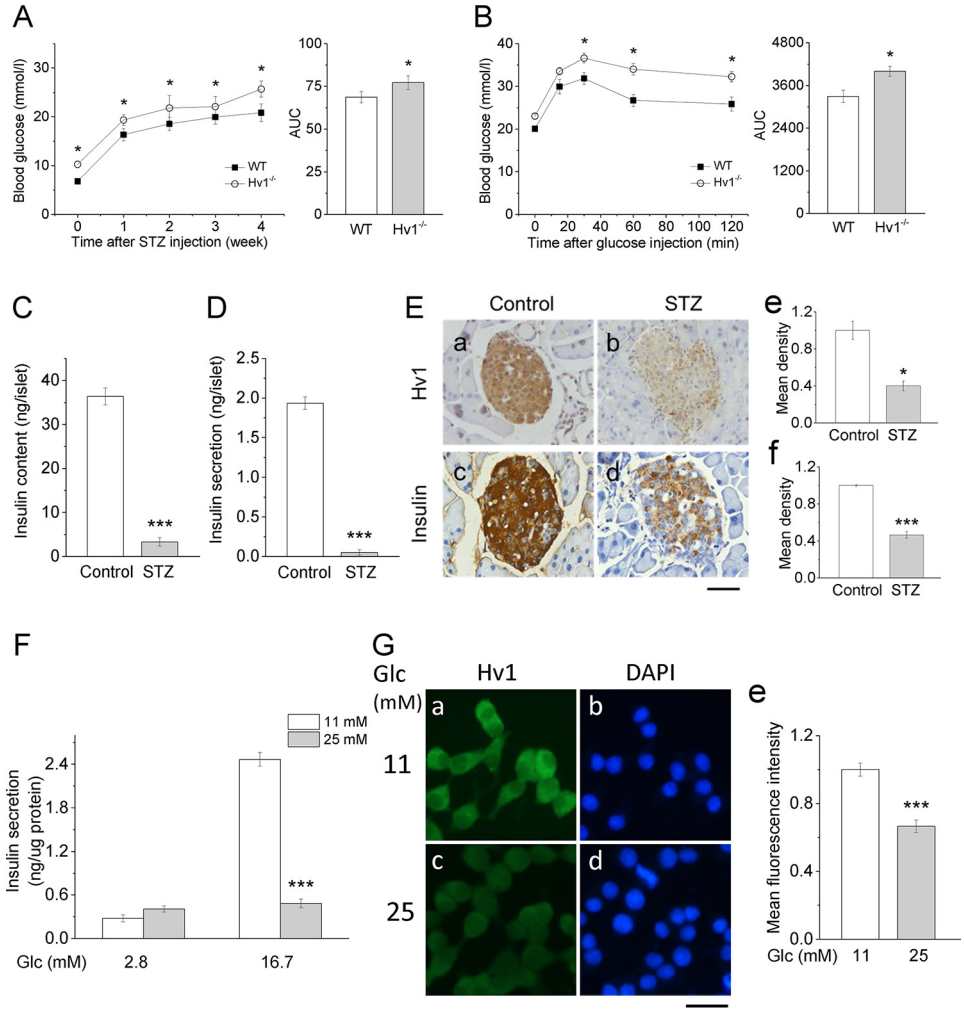

Figure 7. Down-regulation of Hv1 in islets of the STZ-induced diabetes model and glucose-induced dysfunctional β-cells. *A*, basal blood glucose concentrations after fasting for 6 h in STZ-treated KO and WT mice ($n = 23$ for WT; $n = 27$ for KO). Data are mean ± S.E. *, $p < 0.05$; KO *versus* WT. *B*, blood glucose levels measured in whole blood following i.p. injection of glucose (2 g/kg of body weight) in STZ-treated KO and WT mice ($n = 12$ for WT; $n = 14$ for KO). Data are means ± S.E. *, $p < 0.05$; KO *versus* WT. *C*, insulin contents under basal conditions (2.8 mM glucose) in islets isolated from control and STZ-treated WT mice ($n = 10$/genotype). Data are means ± S.E. ***, $p < 0.001$; STZ *versus* control. *D*, 16.7 mM glucose-induced insulin secretion of islets isolated from control and STZ-treated WT mice ($n = 8$/genotype). Data are means ± S.E. ***, $p < 0.001$; STZ *versus* control. *E*, immunohistochemical analysis of pancreas from mice treated with STZ (*b* and *d*) or saline (*a* and *c*, control) using anti-Hv1 and anti-insulin monoclonal antibodies and representative images of anti-Hv1 (*a* and *b*) and anti-insulin (*c* and *d*) antibody-stained pancreatic sections. *Scale bar* = 50 μm. Mean optical density of Hv1- and insulin-positive areas of islets of control and STZ-treated WT mice (*e*, *Hv1*, *top*; *f*, *insulin*, *bottom*). Twenty to thirty sections per pancreas were analyzed ($n = 8$/condition). Data are means ± S.E. *, $p < 0.05$; ***, $p < 0.001$; STZ *versus* control. Hv1 is down-regulated in pancreatic islets in STZ-induced diabetic mice. *F*, Glucose-induced insulin secretion from INS-1 (832/13) cells chronically incubated at 11 (control) and 25 mM glucose for 48 h. Data are means ± S.E. ($n = 8$ per condition). ***, $p < 0.001$, vs. control. *G*, Immunofluorescence analysis of INS-1 (832/13) cells chronically incubated at 11 (control) and 25 mM glucose for 48 h using anti-Hv1 monoclonal antibody. Representative images of anti-Hv1 monoclonal antibody-stained INS-1 (832/13) cells (*a* and *c*) and DAPI stain to visualize the nuclei (*b* and *d*). Scale bar, 20 μM. Mean fluorescence intensity of Hv1-positive area of the cells (*e*), expressed as an average of five experiments (Five different perspectives were counted per experiment. 50–150 cells per perspective). Data are means ± S.E. ***, $p < 0.001$, vs. control. Hv1 is also obviously down-regulated in dysfunctional INS-1 (832/13) cells.

have been observed for glucokinase (32). Hv1 expression levels are significantly decreased in β-cells of STZ-treated diabetes mice and mice with chronic hyperglycemia–induced dysfunction. These data further confirm that Hv1 is closely related to insulin secretion. The findings of this study clearly demonstrate that Hv1 plays an important role in positively regulating GSIS.

β-Cell failure is associated with not only decreased β-cell insulin secretory function but also reduced overall β-cell mass (33). In this study, there was no difference in islet morphology between KO and WT mice and only a very modest decrease in islet size and β-cell mass. The smaller size of Hv1-deficient pancreatic islets may be related to the decrease in β-cell mass and result from impaired insulin secretion function. It is important to note that, *in vitro*, siRNA-mediated knockdown of Hv1 in isolated islets and INS-1 (832/13) cells caused decreased GSIS (17), suggesting that the *in vivo* decrease in insulin secretion in KO mice was not due to an *in vivo* β-cell developmental defect.

Glucose metabolism generates ATP and closes ATP-regulated K^+ channels, leading to membrane depolarization. Membrane depolarization of β-cells leads to activation of voltage-sensitive L-type Ca^{2+} channels with a subsequent rise in intracellular Ca^{2+}, which then drives vesicular exocytosis (34). Sulfonylureas, such as tolbutamide and glibenclamide, bind to the SUR subunit of ATP-sensitive K^+ channels and induce channel closure (35). Knockout of Hv1 inhibits tolbutamide-

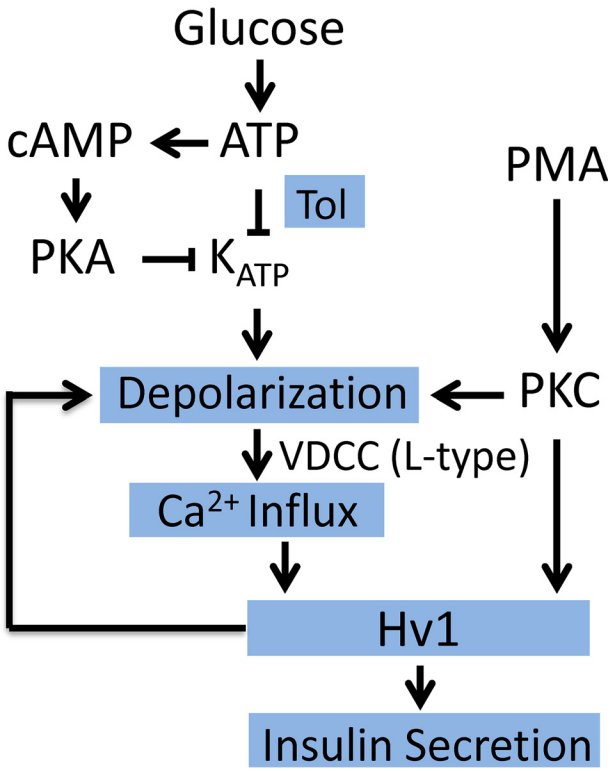

Figure 8. Proposed operation of the voltage-gated proton channel Hv1 on signal transduction pathways of insulin secretion stimulation.

and glibenclamide-induced insulin secretion (data not shown), suggesting that the effect of Hv1 on insulin secretion is downstream of ATP-sensitive K^+ channel closure but upstream of the final exocytotic event.

PMA is a well-known Hv1 activator (13, 14). Our results show that loss of Hv1 strikingly inhibits PMA-stimulated insulin secretion, demonstrating that PMA regulates insulin secretion by activating Hv1 activity. PMA treatment results in a decrease in cytosolic pH in Hv1-deficient β-cells, suggesting that Hv1 is involved in regulating cytosolic pH. It is noteworthy that Hv1-deficiet neutrophils were acidified upon stimulation with PMA, which indicates that Hv1 extrudes the acid generated in the cytosol during activation of neutrophils by PMA (15). It is possible that a similar mechanism exists in islets. Glucose metabolism accompanies proton generation, and therefore, β-cells must have a dynamic intracellular pH-regulatory system (9). The requirement of Hv1 for insulin secretion in islet β-cells suggests that pH regulation is a link in stimulus–secretion coupling in β-cells. pH regulation in pancreatic islets and β-cells in response to glucose might be mainly due to activation of Hv1.

The proposed mechanism of Hv1 in signal transduction pathways relevant to glucose- and PMA-induced insulin secretion is shown in Fig. 8. Glucose metabolism generates ATP and results in depolarization of the plasma membrane because of closure of ATP-sensitive K^+ channels (K_{ATP} channels) (36). Depolarization leads to Ca^{2+} influx through voltage-dependent Ca^{2+} channels (6), opens the Hv1 channel that affects the oscillations in membrane potential (V_m) and cytosolic Ca^{2+} levels in the feedback path, and then triggers insulin exocytosis. ATP is also converted into cAMP and activates PKA and also leads to closure of K_{ATP} channels. PMA, as an Hv1 activator, activates PKC (26) and opens Hv1, resulting insulin secretion. The important defect that ablates the Hv1 gene could be predicted from the reduced depolarization in β-cells and the reduced ability of glucose to raise the level of Ca^{2+} in islets, as we observed in this work. Without activation of Hv1, depolarization by closure of the K_{ATP} channel might be weakened a lot, and these distal effects could not occur.

Blood glucose control is a complex metabolic process involving numerous tissues and organs. Global knockout of Hv1 might affect glucoregulation in many tissues and organs. Insulin is the only hypoglycemic hormone secreted from pancreatic β-cells. Hv1 is highly expressed in pancreatic β-cells (17). Knockout of Hv1 remarkably reduces glucose-stimulated insulin secretion in isolated islets and serum insulin levels in mice, suggesting that hyperglycemia and glucose intolerance in Hv1KO mice are due to decreased insulin secretion in pancreatic β-cells. The decreased insulin and Hv1 expression in pancreatic islets in diabetes model mice imply a link of Hv1 with insulin secretion and diabetes. Taken together, the data in this study demonstrate that Hv1-deficient mice exhibit hyperglycemia and impaired glucose tolerance because of reduced insulin secretion. This finding provides direct evidence of a functional role of the proton channel in maintenance of glucose homeostasis. This study describes a novel pathway regulating β-cell secretory function in which Hv1 sustains entry of calcium ions into β-cells by regulating membrane depolarization to promote increased insulin secretion responses.

Experimental procedures

Animals and treatments

Mice bearing a targeted disruption in the VSOP/Hv1 (VSOP/$Hv1^{-/-}$, backcrossed eight times, kindly provided by Dr. Y. Okamura, School of Medicine, Osaka University), as described previously (37). WT mice (VSOP/$Hv1^{+/+}$) were of the same genetic background (C57BL/6J). Animals were kept in a pathogen-free facility under a 12-h light/dark cycle with access to water and a standard mouse diet (Lillico Biotechnology). Genotyping was performed by PCR as described by Ramsey *et al.* (25). Experiments were performed with 2- to 4-month-old male mice unless indicated otherwise. All animal husbandry and experiments were approved by and performed in accordance with guidelines from the Animal Research Committee of Nankai University.

Blood glucose and insulin determination

Blood glucose levels were measured from blood obtained from the tail vein after fasting for 6 h using an automated glucometer (One Touch, Johnson & Johnson). For glucose tolerance tests, mice 4 months of age were fasted for 6 h before i.p. injection of glucose (2 g/kg of body weight), and blood glucose concentration was measured 0, 15, 30, 60, and 120 min after injection. For insulin tolerance tests, mice were fasted for 6 h before intraperitoneal injection with insulin (1.0 units/kg of body weight), and blood glucose concentration was measured at 0, 15, 30, 60, and 120 min.

For serum insulin measurements, glucose (2 g/kg of body weight) was injected i.p. Venous blood was collected at 0, 2, 5,

15, and 30 min in chilled heparinized tubes and immediately centrifuged, and the serum was stored at −80 °C. Insulin levels were measured by ELISA (Mercodia).

Isolation of pancreatic islets

Pancreatic islets were isolated according to the collagenase digestion method described by Lacy and Kostianovsky (38), with slight modifications. Krebs–Ringer bicarbonate HEPES (KRBH) buffer (135 mM NaCl, 3.6 mM KCl, 5 mM $NaHCO_3$, 0.5 mM NaH_2PO_4, 0.5 mM $MgCl_2$, 1.5 mM $CaCl_2$, and 10 mM HEPES (pH 7.4)) was used for islet isolation. Isolated islets were cultured overnight in RPMI 1640 medium (Gibco) containing 10% FBS in a humidified 5% CO_2 atmosphere at 37 °C before hand-picking for experiments as described previously (17).

Insulin secretion assay

Insulin secretion from isolated islets was measured as described previously (17). Briefly, after overnight culture, the islets were aliquoted into microtubes (20 size-matched islets/tube) and preincubated for 1 h in KRBH-BSA buffer containing 2.8 mM glucose at 37 °C. Then the islets were incubated with different stimuli in KRBH-BSA buffer for 1.5 h. To measure biphasic insulin secretion, islets were first stabilized for 30 min in KRBH-BSA buffer containing 2.8 mM glucose at 37 °C. Following establishment of a baseline with 2.8 mM glucose in KRBH-BSA buffer for 10 min, islets were picked by hand and plated into KRBH-BSA buffer containing 16.7 mM glucose for 10 min and then in another dish for 20 min. Insulin levels in fractions were measured. Islet perifusion was performed at 37 °C using a system designed in-house. Forty equal size islets were paired between WT and KO mice in each experiment. Islets were perifused with KRBH-BSA buffer. The flow rate was controlled by a perfusion pump at 500 μl/min, and fractions were collected in microtubes for insulin determination. Total insulin and proinsulin content in isolated islets was extracted with acidic ethanol and determined using rat/mouse proinsulin and mouse and rat insulin ELISA (Mercodia) according to the manufacturer's protocol.

Immunohistochemistry

Immunohistochemistry was performed as described previously (17).

Transmission EM (TEM)

Islets isolated from six 4-month-old animals were fixed in 2.5% glutaraldehyde for ultrathin (70 nm) sectioning and imaging by TEM (Hitachi HT7700). For quantification of vesicles, images were captured using TEM at magnification ×10,000–15,000. Docked vesicles were counted, with vesicles whose outer surface was within 100 nm of the plasma membrane considered docked granules. At least 50 random sections were used to capture microscopic fields from six mice per group. Then about 50 cells of each genotype were analyzed before identifying their genotype.

Western blotting

Western blotting was performed with anti-α-tubulin (Developmental Studies Hybridoma Bank), anti-VAMP2 (Proteintech), anti-Stx1A (Synaptic Systems), and anti-Syt7 (Synaptic Systems), with final dilutions of 1:1000, 1:500, 1:1000, and 1:250, respectively, as described earlier (39). The intensity of individual bands was quantified using ImageJ software. Each experiment was performed in triplicate.

Measurements of intracellular Ca^{2+}

Isolated islets were incubated in KRBH buffer with basal glucose containing 2 μM Fura-2/AM dye (Invitrogen) for 30 min at 37 °C. The glass coverslips were placed on the stage of an inverted microscope (Eclipse Ti, Nikon). Epifluorescence mode with a ×10 objective was used, stepping to 340 nm excitation and 380 nm excitation for 100 ms every 3 s. Regions of interest were outlined and monitored simultaneously during the whole experimental procedure using MetaFluor software. The resultant fluorescent signals of Fura-2 were successfully monitored at a wavelength of 535 nm with the help of a digital CMOS camera (Zyla 4.2 Plus, Undor). Individual images and intensity values were recorded along with the emission data. After data acquisition, an area of the coverslip without cells was measured as background. Background fluorescence was then subtracted, and the ratio of emission with 340 nm excitation to emission with 380 nm excitation was calculated, showing the F340/F380 ratio for real-time intensity measurements.

Measurements of membrane potential

The voltage-sensitive bisoxonol fluorescent dye DiBAC4(3) was used to study the membrane potential changes of dispersed islet β-cells. Freshly isolated mouse islets were dispersed at room temperature into single cells by addition of 0.1% trypsin-EDTA solution for 2 min with gentle pipetting. The dispersed cells were washed with RPMI 1640 medium containing 10% FBS and placed on 0.01% poly-L-lysine–precoated glass coverslips for 12 h before experiments. The cells were incubated with 1 μM DiBAC4(3) for 30 min at 37 °C in basal glucose in KRBH buffer prior to fluorescence measurement. Data were expressed as an average of three experiments (80–100 cells/experiment).

Measurements of cytosolic pH

Cytosolic pH (pH_c) was assessed using BCECF/AM (Invitrogen) as described previously (40). β-Cells seeded on glass coverslips were loaded with 2 μg/ml of BCECF-AM (Molecular Probes) at 37 °C for 30 min, inserted in a thermostatic chamber, and imaged through a ×10 objective. To determine the cytosolic pH, fluorescence at excitation wavelengths of 436 and 495 nm was recorded at an emission wavelength of 535 nm. Calibration of fluorescence *versus* pH was performed by equilibration of external and internal pH with nigericin (10 μM) in a high K^+ buffer with a pH range of 5.5 to 8.0. High-K^+ buffer contained 145 mM KCl, 2.8 mM glucose, 1 mM $CaCl_2$, 1 mM $MgCl_2$, and 20 mM HEPES (or MES). The relative fluorescence ratio values were plotted against corresponding pH_c values, which allowed determination of the unknown pH_c. The data were expressed as an average of three experiments (50–100 cells/experiment). To observe the change in cytosolic pH induced by PMA (an activator of Hv1), fluorescence at an excitation wavelength of 488 nm was recorded at an emission wavelength of 535 nm. Analysis was performed with MetaMorph software. To exclude any contribution of the Na^+/H^+ antiporter, experi-

ments were performed in Na^+-free medium containing 121 mM N-Methyl-D-glucaMine-Cl, 5.6 mM KCl, 1.2 mM $MgCl_2$, 2.6 mM $CaCl_2$, 5 mM HEPES, and 5 mM glucose (pH 7.4). The changes in cytosolic pH were estimated as the relative changes of the initial fluorescence intensity (F/F_0). The data were expressed as an average of three experiments (20–30 cells/experiment).

Streptozotocin (STZ) diabetes model

To induce diabetes, WT and $Hv1^{-/-}$ mice were treated with STZ (50 mg/kg of body weight i.p. for 5 consecutive days). Additionally, some WT and $Hv1^{-/-}$ mice were treated with saline as vehicle controls. Blood glucose levels were measured once every week with fasting for 6 h after the final injection of STZ. At the end of the fourth week, an IPGTT was performed, using an i.p. injection of glucose at 2 g/kg of body weight after 6 h of fasting. Blood glucose was analyzed 0, 15, 30, 60, and 120 min after introducing glucose. Diabetic hyperglycemia was defined as a fasting blood glucose concentration of more than 11.1 mM for two or more consecutive tests.

Cell culture

The pancreatic islet β-cell line INS-1 (832/13) was obtained from Dr. Hans Hohmeier (Duke University) and grown in RPMI 1640 medium (Gibco) supplemented with 10% FBS, 2 mM glutamate, 1 mM sodium pyruvate, and 55 μM β-mercaptoethanol in a humidified 5% CO_2 atmosphere at 37 °C.

siRNA silencing

To down-regulate Hv1 expression level in INS-1 (832/13) cells, siRNA targeting the Hv1 gene (5′-CTACAAGAAATGGGAGAAT-3′) and a scramble sense sequence (5′-TTCTCCGAACGTGTCACGT-3′), obtained from Ribobio (Guangzhou, China), were used as described previously (17).

Statistical analysis

All statistics were performed using SPSS20.0 software. Comparison of the mean between groups was performed by *t* test. $p < 0.05$ was considered significant.

Author contributions—H. P. and S. J. L. conceptualization; H. P., X. W., S. Z., W. X., J. L., J. Q., Q. Z., and S. J. L. data curation; H. P., X. W., S. Z., W. X., J. L., Q. Z., L. C., and S. J. L. software; H. P., X. W., S. Z., W. X., J. Q., Q. Z., Y. C., L. C., and S. J. L. formal analysis; H. P., X. W., S. Z., J. L., J. Q., Q. Z., and S. J. L. investigation; H. P., X. W., S. Z., W. X., J. L., and J. Q. visualization; H. P., X. W., S. Z., W. X., J. L., Q. Z., Y. C., L. C., and S. J. L. methodology; H. P. and S. J. L. writing-original draft; S. Z., L. C., and S. J. L. validation; Y. C., L. C., and S. J. L. resources; Y. C. and L. C. supervision; L. C. and S. J. L. writing-review and editing; S. J. L. funding acquisition; S. J. L. project administration.

Acknowledgments—We thank Dr. Claes B. Wollheim and Dr. Nicolas Demaurex (Department of Cell Physiology and Metabolism, University of Geneva) for reviewing the manuscript and many helpful discussions. We also thank Dr. Y. Okamura (School of Medicine, Osaka University) for providing VSOP/Hv1 KO mice, Dr. Hans E. Hohmeier (Duke University Medical Center) for providing materials, and Dr. Yifan Wang for reading the manuscript and useful advice.

References

1. Ashcroft, F. M., and Rorsman, P. (2012) Diabetes mellitus and the β cell: the last ten years. *Cell* **148,** 1160–1171 CrossRef Medline
2. Cerasi, E. (1975) Mechanisms of glucose stimulated insulin secretion in health and in diabetes: some re-evaluations and proposals. *Diabetologia* **11,** 1–13 CrossRef Medline
3. Curry, D. L., Bennett, L. L., and Grodsky, G. M. (1968) Dynamics of insulin secretion by the perfused rat pancreas. *Endocrinology* **83,** 572–584 CrossRef Medline
4. Nunemaker, C. S., Wasserman, D. H., McGuinness, O. P., Sweet, I. R., Teague, J. C., and Satin, L. S. (2006) Insulin secretion in the conscious mouse is biphasic and pulsatile. *Am. J. Physiol. Endocrinol. Metab.* **290,** E523–E529 CrossRef Medline
5. Hosker, J. P., Rudenski, A. S., Burnett, M. A., Matthews, D. R., and Turner, R. C. (1989) Similar reduction of first- and second-phase B-cell responses at three different glucose levels in type II diabetes and the effect of gliclazide therapy. *Metabolism* **38,** 767–772 CrossRef Medline
6. Rorsman, P., and Renström, E. (2003) Insulin granule dynamics in pancreatic β cells. *Diabetologia* **46,** 1029–1045 CrossRef Medline
7. Henquin, J. C., Ishiyama, N., Nenquin, M., Ravier, M. A., and Jonas, J. C. (2002) Signals and pools underlying biphasic insulin secretion. *Diabetes* **51,** S60–67 CrossRef Medline
8. Shibasaki, T., Takahashi, H., Miki, T., Sunaga, Y., Matsumura, K., Yamanaka, M., Zhang, C., Tamamoto, A., Satoh, T., Miyazaki, J., and Seino, S. (2007) Essential role of Epac2/Rap1 signaling in regulation of insulin granule dynamics by cAMP. *Proc. Natl. Acad. Sci. U.S.A.* **104,** 19333–19338 CrossRef Medline
9. Pace, C. S., Tarvin, J. T., and Smith, J. S. (1983) Stimulus-secretion coupling in β-cells: modulation by pH. *Am. J. Physiol.* **244,** E3–E18 Medline
10. Lindström, P., and Sehlin, J. (1984) Effect of glucose on the intracellular pH of pancreatic islet cells. *Biochem. J.* **218,** 887–892 CrossRef Medline
11. Lindström, P., and Sehlin, J. (1986) Effect of intracellular alkalinization on pancreatic islet calcium uptake and insulin secretion. *Biochem. J.* **239,** 199–204 CrossRef Medline
12. Barg, S., Huang, P., Eliasson, L., Nelson, D. J., Obermüller, S., Rorsman, P., Thévenod, F., and Renström, E. (2001) Priming of insulin granules for exocytosis by granular Cl- uptake and acidification. *J. Cell Sci.* **114,** 2145–2154 Medline
13. Ramsey, I. S., Moran, M. M., Chong, J. A., and Clapham, D. E. (2006) A voltage-gated proton-selective channel lacking the pore domain. *Nature* **440,** 1213–1216 CrossRef Medline
14. Sasaki, M., Takagi, M., and Okamura, Y. (2006) A voltage sensor-domain protein is a voltage-gated proton channel. *Science* **312,** 589–592 CrossRef Medline
15. El Chemaly, A., Okochi, Y., Sasaki, M., Arnaudeau, S., Okamura, Y., and Demaurex, N. (2010) VSOP/Hv1 proton channels sustain calcium entry, neutrophil migration, and superoxide production by limiting cell depolarization and acidification. *J. Exp. Med.* **207,** 129–139 CrossRef Medline
16. Lishko, P. V., Botchkina, I. L., Fedorenko, A., and Kirichok, Y. (2010) Acid extrusion from human spermatozoa is mediated by flagellar voltage-gated proton channel. *Cell* **140,** 327–337 CrossRef Medline
17. Zhao, Q., Che, Y., Li Q., Zhang, S., Gao, Y. T., Wang, Y., Wang, X., Xi, W., Zuo, W., and Li, S. J. (2015) The voltage-gated proton channel Hv1 is expressed in pancreatic islet β-cells and regulates insulin secretion. *Biochem. Biophys. Res. Commun.* **468,** 746–751 CrossRef Medline
18. Matthews, D. R., Hosker, J. P., Rudenski, A. S., Naylor, B. A., Treacher, D. F., and Turner, R. C. (1985) Homeostasis model assessment: insulin resistance and β-cell function from fasting plasma glucose and insulin concentrations in man. *Diabetologia* **28,** 412–419 CrossRef Medline
19. Lang, J. (1999) Molecular mechanisms and regulation of insulin exocytosis as a paradigm of endocrine secretion. *Eur. J. Biochem.* **259,** 3–17 CrossRef Medline
20. Zhao, A., Ohara-Imaizumi, M., Brissova, M., Benninger, R. K., Xu, Y., Hao, Y., Abramowitz, J., Boulay, G., Powers, A. C., Piston, D., Jiang, M., Nagamatsu, S., Birnbaumer, L., and Gu, G. (2010) Gαo represses insulin secretion by reducing vesicular docking in pancreatic β-cells. *Diabetes* **59,** 2522–2529 CrossRef Medline

21. Jahn, R., and Scheller, R. H. (2006) SNAREs: engines for membrane fusion. *Nat. Rev. Mol. Cell Biol.* **7,** 631–643 CrossRef Medline
22. Gustavsson, N., Lao, Y., Maximov, A., Chuang, J. C., Kostromina, E., Repa, J. J., Li, C., Radda, G. K., Südhof, T. C., and Han, W. (2008) Impaired insulin secretion and glucose intolerance in synaptotagmin-7 null mutant mice. *Proc. Natl. Acad. Sci. U.S.A.* **105,** 3992–3997 CrossRef Medline
23. Qureshi, F. M., Dejene, E. A., Corbin, K. L., and Nunemaker, C. S. (2015) Stress-induced dissociations between intracellular calcium signaling and insulin secretion in pancreatic islets. *Cell Calcium* **57,** 366–375 CrossRef Medline
24. Dula, S. B., Jecmenica, M., Wu, R., Jahanshahi, P., Verrilli, G. M., Carter, J. D., Brayman, K. L., and Nunemaker, C. S. (2010) Evidence that low-grade systemic inflammation can induce islet dysfunction as measured by impaired calcium handling. *Cell Calcium* **48,** 133–142 CrossRef Medline
25. Ramsey, I. S., Ruchti, E., Kaczmarek, J. S., and Clapham, D. E. (2009) Hv1 proton channels are required for high-level NADPH oxidase-dependent superoxide production during the phagocyte respiratory burst. *Proc. Natl. Acad. Sci. U.S.A.* **106,** 7642–7647 CrossRef Medline
26. Decoursey, T. E. (2003) Voltage-gated proton channels and other proton transfer pathways. *Physiol. Rev.* **83,** 475–579 CrossRef Medline
27. Zhang, C. Y., Parton, L. E., Ye, C. P., Krauss, S., Shen, R., Lin, C. T., Porco, J. A., Jr, and Lowell, B. B. (2006) Genipin inhibits UCP2-mediated proton leak and acutely reverses obesity- and high glucose-induced β cell dysfunction in isolated pancreatic islets. *Cell Metab.* **3,** 417–427 CrossRef Medline
28. Taguchi, N., Aizawa, T., Sato, Y., Ishihara, F., and Hashizume, K. (1995) Mechanism of glucose-induced biphasic insulin release: physiological role of adenosine triphosphate-sensitive K^+ channel-independent glucose action. *Endocrinology* **136,** 3942–3948 CrossRef Medline
29. Gunawardana, S. C., and Sharp, G. W. (2002) Intracellular pH plays a critical role in glucose-induced time-dependent potentiation of insulin release in rat islets. *Diabetes* **51,** 105–113 CrossRef Medline
30. Al-Awqati, Q. (1986) Proton-translocating ATPases. *Annu. Rev. Cell Biol.* **2,** 179–199 CrossRef Medline
31. Burgess, T. L., and Kelly, R. B. (1987) Constitutive and regulated secretion of proteins. *Annu. Rev. Cell Biol.* **3,** 243–293 CrossRef Medline
32. Matschinsky, F. M., Glaser, B., and Magnuson, M. A. (1998) Pancreatic β-cell glucokinase: closing the gap between theoretical concepts and experimental realities. *Diabetes* **47,** 307–315 CrossRef Medline
33. Weir, G. C., and Bonner-Weir, S. (2004) Five stages of evolving β-cell dysfunction during progression to diabetes. *Diabetes* **53,** S16–S21 CrossRef Medline
34. Barg, S., Ma, X., Eliasson, L., Galvanovskis, J., Göpel, S. O., Obermüller, S., Platzer, J., Renström, E., Trus, M., Atlas, D., Striessnig, J., and Rorsman, P. (2001) Fast exocytosis with few Ca^{2+} channels in insulin-secreting mouse pancreatic B cells. *Biophys. J.* **81,** 3308–3323 CrossRef Medline
35. Proks, P., Reimann, F., Green, N., Gribble, F., and Ashcroft, F. (2002) Sulfonylurea stimulation of insulin secretion. *Diabetes* **51,** S368–S376 CrossRef Medline
36. Aguilar-Bryan, L., and Bryan, J. (1999) Molecular biology of adenosine triphosphate-sensitive potassium channels. *Endocr. Rev.* **20,** 101–135 CrossRef Medline
37. Okochi, Y., Sasaki, M., Iwasaki, H., and Okamura, Y. (2009) Voltage-gated proton channel is expressed on phagosomes. *Biochem. Biophys. Res. Commun.* **382,** 274–279 CrossRef Medline
38. Lacy, P. E., and Kostianovsky, M. (1967) Method for the isolation of intact islets of Langerhans from the rat pancreas. *Diabetes* **16,** 35–39 CrossRef Medline
39. Wang, Y., Wu, X., Li, Q., Zhang, S., and Li, S. J. (2013) Human voltage-gated proton channel Hv1: a new potential biomarker for diagnosis and prognosis of colorectal cancer, *PLoS ONE* **8,** e70550 CrossRef Medline
40. Wang, Y., Li, S. J., Wu, X., Che, Y., and Li, Q. (2012) Clinicopathological and biological significance of human voltage-gated proton channel Hv1 protein overexpression in breast cancer. *J. Biol. Chem.* **287,** 13877–13888 CrossRef Medline